Asian Journal of Andrology (2018) 20, 442–447
www.asiaandro.com; www.ajandrology.com

Open Access

ORIGINAL ARTICLE

Erectile Dysfunction

Nanotechnology-assisted adipose-derived stem cell (ADSC) therapy for erectile dysfunction of cavernous nerve injury: *in vivo* cell tracking, optimized injection dosage, and functional evaluation

Han Wu[1,2,3], Wen-Hao Tang[1,2,3,4], Lian-Ming Zhao[1,2,3], De-Feng Liu[2,3], Yu-Zhuo Yang[2,3,4], Hai-Tao Zhang[1,2,3], Zhe Zhang[1,2,3], Kai Hong[1,2,3], Hao-Cheng Lin[1,2,3], Hui Jiang[1,2,3,4]

Stem cell therapy is a potentially promising option for erectile dysfunction; however, its risk of tumorigenicity is a clinical hurdle and the risk is positively related to the number of injected cells. Our previous study showed that nanotechnology improved adipose-derived stem cell (ADSC) therapy for erectile dysfunction of cavernous nerve injury (CNI) by attracting cells in the corpus cavernosum. These results indicated the possibility of using a reduced dosage of ADSCs for intracavernous injection. In this exploratory study, we used lower dosage (2×10^5 cells) of ADSCs for intracavernous injection (ICI) and the nanotechnology approach. Intracavernous pressure and mean arterial pressure were measured at day 28 to assess erectile function. The low-dose ADSC therapy group showed favorable treatment effects, and nanotechnology further improved these effects. *In vivo* imaging of ICI cells revealed that the fluorescein signals of NanoShuttle-bound ADSCs (NanoADSCs) were much stronger than those of ADSCs at days 0, 1, and 3. Both immunofluorescence and Western blot analysis showed a significant increase in smooth muscle, endothelium, and nerve tissue in the ADSC group compared to that in the CNI group; further improvement was achieved with assisted nanotechnology. These findings demonstrate that nanotechnology can be used to further improve the effect of small dosage of ADSCs to improve erectile function. Abundant NanoADSCs remain in the corpus cavernosum *in vivo* for at least 3 days. The mechanism of erectile function improvement may be related to the regeneration of the smooth muscle, endothelium, and nerve tissues.

Asian Journal of Andrology (2018) **20**, 442–447; doi: 10.4103/aja.aja_48_18; published online: 10 July 2018

Keywords: adipose-derived stem cell (ADSC); cavernous nerve injury; cell tracking; erectile dysfunction

INTRODUCTION

Prostate cancer is one of the most prevalent malignant cancers among the male population.[1] Radical prostatectomy (RP) is the main treatment for localized prostate cancer and has been demonstrated in a randomized controlled trial to reduce the progression to metastases and death from the disease.[2] Erectile dysfunction (ED) is a common postoperative complication of RP and is associated with iatrogenic injury to the cavernous nerve (CN). The morbidity of RP-related ED varies greatly according to the literature (20%–93.9%).[3–5] Interoperative stretching, heating, or crushing are thought to be responsible for direct damage to the neurovascular bundle, and Wallerian degeneration of the CN may result in ED.[6] Currently, several treatment options are available for patients with ED. For patients with CN injury (CNI), erections may fail according to subsequent neuropraxia, ischemia, and corporal fibrosis, limiting the effects of traditional ED treatments.[6]

Adipose tissue-derived stem cells (ADSCs) are the most widely used type of stem cells in ED research because they are easy to obtain from abundant tissue sources.[7] Intracavernous injection (ICI) is the most common ADSC delivery method for ED treatment and has been shown to be effective and practical.[8] However, because the cavernosa has an abundant blood supply, intracavernosal-injected ADSCs are not retained in a specific location *in situ* because of their high blood clearance.[9] A magnetic field-assisted method (nanotechnology) was found in our previous study to retain the cells in the corpus cavernosum (CC),[10] indicating that low-dosage injection can result in effective treatment. However, stem cells injected *in vivo* pose a risk of tumor formation, with the risk positively related to the number of injected cells. Thus, we tested the effect and *in vivo* diffusion of a small-dosage cell injection to determine if fewer cells showed favorable treatment effects while decreasing the risk of tumor formation by staying *in situ* with the help of nanotechnology.

The present study promotes the understanding of ICI-cell diffusion and provides clues for exploring the optimal dosage of ADSC transplantation to treat erectile dysfunction after CNI.

[1]Department of Urology, Peking University Third Hospital, Beijing 100191, China; [2]Department of Reproductive Medicine Center, Peking University Third Hospital, Beijing 100191, China; [3]Department of Andrology, Peking University Third Hospital, Beijing 100191, China; [4]Department of Human Sperm Bank, Peking University Third Hospital, Beijing 100191, China.
Correspondence: Dr. H Jiang (jianghui55@163.com) or Dr. HC Lin (haochenglin292@163.com)
Received: 13 February 2018; Accepted: 04 May 2018

MATERIALS AND METHODS

Animals and grouping

In total, forty-three 12-week-old male Sprague-Dawley (SD) rats were used in this study. All rats were ordered from the Experimental Animal Department, Peking University Health Science Center (PUHSC), Beijing, China. The study was approved by the office of laboratory animal welfare of PUHSC. The approval number is LA2017003.

Forty male SD rats were randomly assigned to four groups as follows: Cont (control group), CNI (bilateral CNI group), ADSC (ADSC-injected group), and nanotechnology-assisted MagADSC (NanoShuttle-bound ADSCs [NanoADSC]-injected group with an external magnetic field). Operations were performed under pentobarbital sodium (3% saline solution, 1 ml kg^{-1}; HWRK Chem Co., Ltd., Beijing, China) anesthesia. After exposing the major pelvic ganglion (MPG) on the bilateral side walls of the prostate, the operation was completed in Cont group rats and the incision was closed. All rats in the CNI, ADSC, and MagADSC groups were subjected to bilateral CN separation and nerve crush (BCNC) to prepare the ED model. Crushed bilateral CNs were formed 5 mm distal to the MPG using a fine hemostat (Weigao Group Medical Polymer Co., Ltd., Weihai, China) for clamping 30 s three times at 30-s intervals (**Supplementary Figure 1a**).

Seven days after BCNC, ICI of 200-μl phosphate-buffered saline (PBS; Thermo Fisher Scientific Inc., Waltham, MA, USA, CNI group) or 200-μl PBS containing approximately 2×10^5 cells (ADSCs for ADSC group and NanoShuttle-magnetized NanoADSCs for MagADSC group) were administered after anesthesia. Subcutaneous implantation of a magnetic rod (**Supplementary Figure 1b** and **1c**) was conducted in the MagADSC group and the rod was removed 24 h later.

Cell culture and flow cytometry measurement

A 12-week-old male SD rat was used to isolate ADSCs. General anesthesia was achieved by intraperitoneal injection of pentobarbital sodium (HWRK Chem Co., Ltd.). Primary cells were acquired as previously described.[10] Cells were cultured in Dulbecco's modified Eagle's medium/F-12 containing 1% antibiotic-antimycotic solution and 10% fetal bovine serum (Life Technologies, Carlsbad, CA, USA) at 37°C in 95% humidity and 5% CO_2. The medium was changed every 2 days.

Cultured cells were analyzed by flow cytometry with a FACScan argon laser cytometer (BD Biosciences, San Jose, CA, USA) to determine whether the cells met the criteria of the joint statement of the International Federation for Adipose Therapeutics and Science and the International Society for Cellular Therapy.[11] Briefly, cultured passage 2 cells were harvested in 0.05% trypsin and washed with PBS (Thermo Fisher Scientific Inc.) and then protected from light and incubated for 30 min in flow cytometry buffer containing APC/Cy7-conjugated anti-rat CD29, APC-conjugated anti-rat CD45, PerCP-conjugated anti-rat CD90 (BioLegend, Inc., San Diego, CA, USA), and PE-Cy7-conjugated anti-rat CD31 (Thermo Fisher Scientific, Inc.). Separate tubes were prepared for each antibody to provide compensation controls. An extra sample tube containing unstained cells was used as a control.

Lentivirus transfection and ICI

Lentivirus (Hanheng Biotec, Inc., Shanghai, China) containing the green-fluorescent protein (*GFP*) and *Luc* genes was administered to passage 2 ADSCs with a multiplicity of infection (MOI) of 10, 50, and 100. The culture medium was changed 24 h later and GFP expression was determined after 48 h with an inverted fluorescence microscope (LSM 710, Carl Zeiss AG, Oberkochen, Germany); the MOI showing the optimal transfection effect was selected.

NanoADSC preparation was conducted as described previously.[10] Briefly, passage 3 cells were cultured to 80% confluence and incubated with NanoShuttle (1 μl per 1×10^4 cells; Nano3D Biosciences, Inc., Houston, TX, USA) overnight. Unbound NanoShuttle particles were removed by washing on the next day, and cells digested and resuspended in PBS were used for ICI.

Digested passage 3 cells were used for ICI. Isoflurane anesthesia was administered as described above; the penis was dragged out from the foreskin after local sterilization and injected with 200 μl PBS (CNI group), 2×10^5 ADSCs, or NanoADSCs in 200 μl PBS (ADSC and MagADSC groups, respectively) into the CC with a 1 ml insulin syringe (B. Braun Medical, Inc., Bethlehem, PA, USA). The injection site was compressed with a cotton swab for 3 min to prevent backflow.

In vivo imaging and erectile function evaluation

Two 12-week-old SD rats injected with ADSCs and NanoADSCs, respectively, were used in this part. *In vivo* imaging was performed using a PerkinElmer *In Vivo* Imaging System (IVIS, PerkinElmer, Inc., Waltham, MA, USA). Inhalation anesthesia was administered before the imaging procedure and luciferin (VivoGlo™ Luciferin, *In Vivo* Grade, Promega Biotech Co., Ltd., Madison, WI, USA) was injected intraperitoneally (10% PBS solution, 1 ml kg^{-1}) before fluorescence imaging. The systemic cell distribution was determined from the signal intensity within a region of interest.

Intracavernous pressure (ICP) and mean arterial pressure (MAP) were measured 4 weeks with PowerLab work station (AD Instruments Co., Ltd., Sydney, Australia) after ICI as previously described. Two tip-curved Chinese acupuncture fine needles (Tianhe Medical Instrument Co., Ltd., Taixing, China) were used to form a double-arm stimulation hook, with their caudal ends connected to a stimulating electrode (**Supplementary Figure 1d**). The hooks were connected to a 1-ml syringe (Weigao Group Medical Polymer Co., Ltd.) needle with a polyethylene-50 tube (Smiths Medical International Co., Ltd., London, UK) and the needle was inserted into the left CC to measure ICP. MAP was recorded by right carotid artery intubation with a polyethylene-50 tube. Briefly, we exposed the right-sided carotid artery and clipped the proximal side with a vascular clamp, and then formed a 1/3rd circle incision on the distal part of the artery, inserted the tube into the artery, and fixed the tube within the artery with a knot. The clamp was removed and the value of MAP was recorded. For electrical stimulation of erection, we hooked the right-sided CN with the stimulating electrode at the proximal side of the former crushed part (3 mm distal to the MPG).

Stimulations were performed at 3 V and 16 Hz, with a duration of 5 ms for 60 s at 5-min intervals between subsequent stimulations. Data for the ICP/MAP ratio, total ICP (area under the erectile curve), and mean ICP during nerve electrostimulation were collected for statistical analysis in each animal.[12]

Western blot and immunohistochemistry

Protein expression of CD31, α-smooth muscle actin (α-SMA), and Tubb3 protein (β III tubulin) was tested to determine protein levels in the endothelium, smooth muscle, and nerve in CC. Primary antibodies (Abcam Co., Ltd., Cambridge, UK) were incubated at 4°C overnight with a polyvinylidene fluoride membrane (Thermo Fisher Scientific Inc.) to which proteins had been transferred. Bound antibodies were detected using goat anti-mouse IgG H&L (IRDye® 800CW) preadsorbed secondary antibodies (LI-COR, Inc., Lincoln, NE, USA; incubated at room temperature for 1 h) and an infrared fluorescence scanning imaging system (LI-COR, Inc.). Data were normalized to the levels of glyceraldehyde-3-phosphate dehydrogenase (GAPDH).

Six-micrometer-thick penile frozen sections were incubated with primary antibodies, including rabbit anti-α-SMA (1:500), mouse anti-β III tubulin (1:200), and mouse anti-CD31 (1:500) overnight at 4°C, followed by Cy3-bound secondary antibody (Abcam Co., Ltd.) working solution (1:1000) for 30 min at room temperature. Nuclei were stained with Hoechst 33342 (Thermo Fisher Scientific Inc.).

Statistical analyses

Statistical analysis was performed using SPSS 24.0 analysis software (SPSS, Inc., Chicago, IL, USA). The Kolmogorov–Smirnov test was used to determine whether the data showed a normal distribution. Analysis of variance and the nonparametric Kruskal–Wallis test were used to detect differences between normally/abnormally distributed data, respectively. Homogeneity of variance was verified by the Levene test. Statistical significance was accepted at $P < 0.05$. Data were presented as the mean ± standard error of the mean (s.e.m.).

RESULTS

Labeling ADSCs with GFP

Cultured passage 3 ADSCs were fibroblast-like cells in the bright field image as described previously (**Figure 1a**).[13,14] Under the exciting light, the GFP signal were clearly captured under the MOI of 100 (**Figure 1b**).

Identification of ADSCs

The percentages of CD29+/CD90+ and CD29+/CD90+/CD31−/CD45− cells were calculated by flow cytometry with digested passage 2 ADSCs. The total number of analyzed cells was 3569, and 2850 cells were positive for CD29 and CD90 expression (79.9%). The CD31−/CD45− cell group accounted for nearly all the cell population (**Figure 2**).

In vivo tracking

In vivo ADSC tracing images showed that ICI cells spread into the bilateral lungs within a short time (**Figure 3a**). The results showed that the fluorescein signal around the CC of NanoADSCs was much stronger than that of ADSCs at days 0, 1, and 3, but sharply decreased at day 7 (**Figure 3a** and **3b**). The signal of bilateral lung area was stronger in ADSC-injected rats compared with magnetic field-assisted NanoADSC-injected rats (**Figure 3c**).

Erectile function evaluation

Pressures within the right-sided carotid artery and CC during electrically stimulated erection were determined 28 days after ICI. Data for the mean ICP, ICP/MAP, and total ICP are shown in **Supplementary Table 1**. These three indicators in the CNI group were significantly lower than those in the Cont group ($P < 0.05$). The ADSC group showed higher levels for these indicators than that of the CNI group ($P < 0.05$) and further improvement was achieved in the MagADSC group compared to that in the ADSC group ($P < 0.05$). Erectile function in the MagADSC group was similar to that in the Cont group (ICP/MAP, $P = 0.218$; mean ICP, $P = 0.091$; total ICP, $P = 0.055$) (**Figure 4**).

Western blot

The Western blot results demonstrated that the expression of β III tubulin and CD31 in the MagADSC group was higher than that in the CNI group ($P < 0.05$) and ADSC group ($P < 0.05$). The expression of α-SMA, β III tubulin, and CD31 in the ADSC group was higher than that in the CNI group ($P < 0.05$). The expression of β III tubulin in the MagADSC group was similar to that in the Cont group ($P = 0.055$). The ADSC and MagADSC groups showed similar expression levels of α-SMA ($P = 0.228$) (**Figure 5**).

Immunohistochemistry

The ADSC group showed larger Cy3-positive stained areas than the CNI group ($P < 0.05$). Areas positively stained for β III tubulin in the MagADSC group were larger than those in the CNI group ($P < 0.05$) and ADSC group ($P < 0.05$) and similar to that in the Cont group ($P = 0.746$). The CD31 content in the MagADSC group was higher than that in the ADSC group ($P < 0.05$) and CNI group ($P < 0.05$), but α-SMA content was similar to that in the ADSC group ($P = 0.816$). The Cont group showed larger areas of α-SMA and CD31 positively stained areas than the MagADSC group ($P < 0.05$) (**Figure 6**).

DISCUSSION

Penile erection is a complex process based on multisystem coordination. Any damage to the system may lead to ED. Most traditional treatment methods are limited for treating ED resulting from certain types of tissue damage.

Studies of stem cells show promise for improving the understanding of the mechanism of tissue regeneration after injury. Studies applying these techniques have begun to establish a foundation for iatrogenic ED treatment after CNI.[7,15,16] In our previous study, a magnetic field-assisted nanoparticle binding method was developed to extend the retention time of injected ADSCs in the CC.[10] While the dynamic distribution of injected cells after ICI has not yet been clarified. In addition, the underlying mechanisms of injured tissue regeneration remain unclear. The present study tested the effects of small-dose ADSCs ICI for treating ED after BCNC and the cell distribution in living rats. Our structural and molecular data revealed improvements in erectile function.

The mechanism by which stem cells aid in wound healing was unclear.[17] In the ED treatment field, Albersen *et al*.[18] reported that both ADSCs and their lysates improve the recovery of erectile function after CNI. Zhu *et al*.[19] determined the fate of transplanted ADSCs and found that these cells did not express smooth muscle cell markers or endothelial cell markers. In the present study, stronger signals of NanoADSCs in CC compared to ADSCs were observed by *in vivo* imaging at days 0, 1, and 3 after injection, indicating that the use of nanotechnology granted more chance for which NanoADSCs remained in the CC and provided additional possibilities for the cells to exert their functions in tissue regeneration. In contrast, we also found that in both ADSC- and NanoADSC-injected rats, the signals became untrackable after 7 days, suggesting that the injected cell population was decreased during the 1st week after injection. Combined with the results of previous studies, it appears that several weeks are required before ADSCs differentiate into certain cell types,[20–23] and that cell differentiation may not be the major mechanism of tissue regeneration during the 1st week. Second, retaining more cells in the CC would increase the concentration of secreted factors, including cytokines and exosomes enriched with bioactive miRNA and tRNA species,[24] which may explain why the MagADSC group showed the greatest functional improvement.

In the past, because of the lack of effective strategies for tracking cells continuously after *in vivo* injection in living animals, researchers have only observed the cell colonization, distribution, and differentiation in harvested target tissue at different time points. In the present study, we used ADSCs expressing luciferase and its reaction with luciferin as an *in vivo* biomarker to track the cells. Soon after ICI, we detected the fluorescein signal in the bilateral lung area, which agrees with the results of previous studies, showing that soon after transplantation, injected cells disperse into the distal area from the original injection site because of the hypervascular nature of the CC.[9,25] Notably, although distribution occurred soon after injection, the site around CC showed the strongest signal among all the parts of

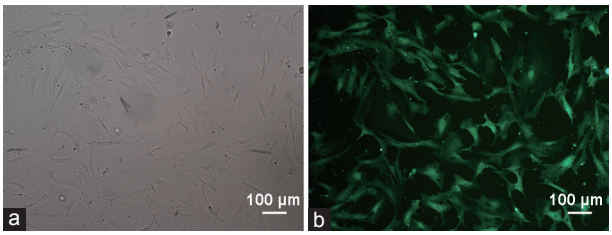

Figure 1: Morphology of cultured ADSC- and GFP-positive cells. (**a**) Passage 3 ADSCs were in fibroblast-like shape. (**b**) Fluorescence images of passage 3-infected ADSCs at an MOI of 100. Scale bars = 100 μm. ADSC: adipose-derived stem cell; MOI: multiplicity of infection; GFP: green-fluorescent protein.

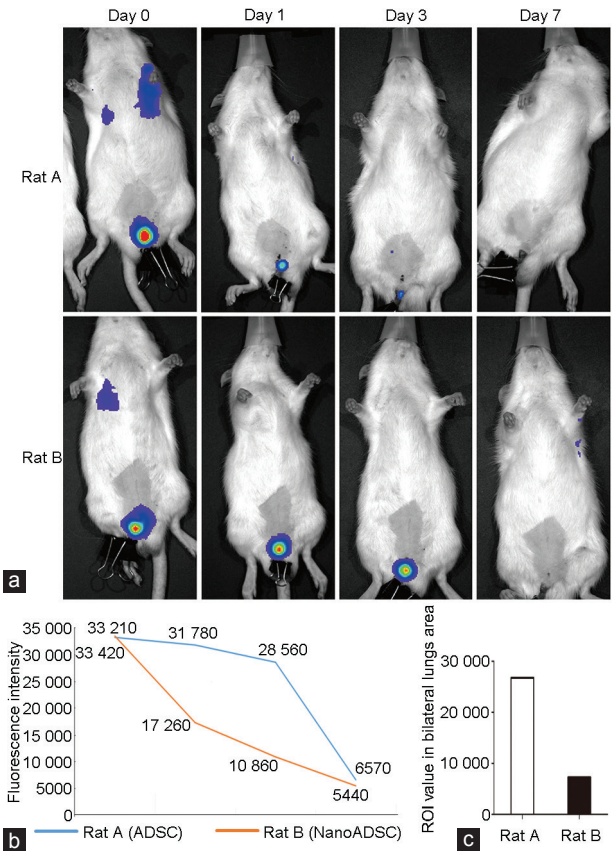

Figure 3: *In vivo* imaging. (**a**) *In situ* colonization of 2 × 10^5 injected cells (by measuring signal within the ROIs) on rat injected with ADSCs and without peri-penis magnetic field (Rat A) and NanoADSC-injected rat with assisted magnetic field (Rat B) at days 0, 1, 3, and 7. (**b**) Clear decreases in fluorescence signal were observed in both rats, and the trend was more moderate in Rat B. (**c**) Signal of bilateral lung area in Rat A was higher than that in Rat B on day 0. ADSC: adipose-derived stem cell; NanoADSCs: NanoShuttle-bound ADSCs; ROI: region of interest.

the body, indicating that ICI is an effective method for retaining cells at their original injection site. The data showed the bioluminescence signal captured around the penis of two rats which exhibited attenuation, but as shown in **Figure 3**, there was a mild decline of the signal in NanoADSCs injected rat, suggesting that nanotechnology can help transplanted cells remain at the injection site *in situ*.

There is no consensus regarding how many cells should be used in a single injection to treat CNI-related ED, and most studies have used millions of cells and shown positive effects.[10,26–28] However,

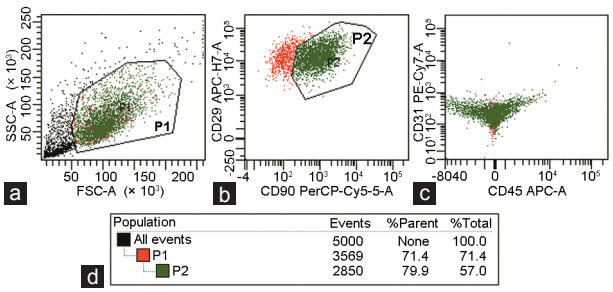

Figure 2: Cytometry analysis of the cultured passage 2 ADSC suspension. (**a**) SSC and FSC of cell suspension detected by flow cytometry, P1-enclosed suspicious cells. (**b**) P2-enclosed cells positively stained with CD29 and CD90. (**c**) Few cells positively stained with CD31 and CD45 were detected. (**d**) The percentage of target cells within P1 and P2 boxes. ADSC: adipose-derived stem cell; SSC: side scatter; FSC: forward scatter; A: area. P1: box enclosed cells except debris; P2: box enclosed CD29 and CD90 double positive cells among P1 box.

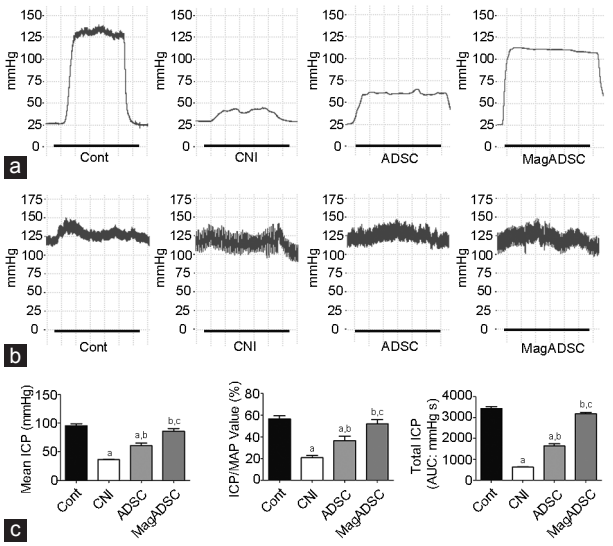

Figure 4: Erectile function evaluation. (**a**) Curves of ICP during erection under electrostimulation of the CN; black lines represent the stimulation window of 1 min. (**b**) Pressures of the carotid artery in each group. (**c**) Bar graphs show the values of mean ICP, ICP/MAP, and total ICP in response to cavernous nerve stimulation on day 28. $^aP < 0.05$, other groups versus Cont group. $^bP < 0.05$, other groups versus CNI group. $^cP < 0.05$, other groups versus ADSC group. Cont: control; CNI: cavernous nerve injury; ADSC: adipose-derived stem cell; MagADSC: magnetic field-assisted nanotechnology-treated ADSC; ICP: intracavernous pressure; MAP: mean arterial pressure.

tumorigenicity is a limitation of pluripotent stem cell therapies, and the potential risk is positively correlated with the number of stem cells used.[29,30] Thus, based on our previous research,[10] we reduced the number of injected cells from 1 × 10^6 to 2 × 10^5; functional evaluation still showed an effective improvement in erectile function in treated rats, and nanotechnology further improved these treatment effects (**Figure 4**). The signal in the lungs was weaker in NanoADSCs injected rat than in ADSCs injected rat, indicating that fewer ADSCs were transferred to the distal part of the living animal once nanotechnology had been used (**Figure 3c**). We predicted that a low dose of injected stem cells would decrease the probability of cell transfer. The nanotechnology restraining ICI stem cells in the penis, that makes fewer stem cells transferred into other part of the body, and that is how the nanotechnology decrease the risk of stem cell related tumorigenicity.

Our immunofluorescence and Western blot results revealed that the content of smooth muscle, endothelium, and nerve in the CC was significantly increased 4 weeks after ADSC-ICI, and nanotechnology further improved these effects. We found that smooth muscle content in the MagADSC group was similar to that in the ADSC group, while β III tubulin content was similar to that in the Cont group, suggesting that low-dose NanoADSCs are superior for nerve regeneration but have a limited ability to regenerate smooth muscle. A study by Fandel *et al.*[31] showed that the damaged nerve may release chemokines to attract stem cells to migrate to the injured site. In the present study, CNI was the original damage factor, which may explain why the restoration effect was more obvious in nerve regeneration. In general, small-dose ADSC-ICI alleviated ED of CNI and nanotechnology further improved the treatment effect by retaining more cells in the CC and promoting smooth muscle, endothelium, and nerve regeneration.

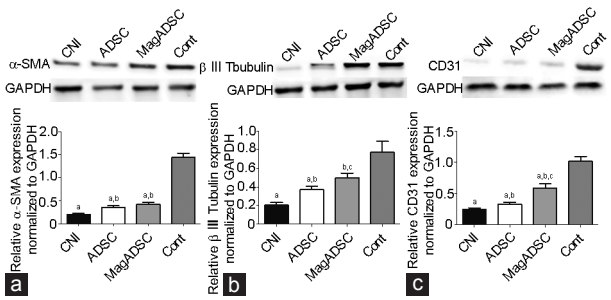

Figure 5: Protein expression at the four groups on day 28, as evaluated by Western blot analysis. (**a**) α-SMA expression. (**b**) Protein expression of β III tubulin in rat penis from different groups. (**c**) CD31 expression in each group. Intergroup differences were evaluated by independent *t*-test. $^{a}P < 0.05$, other groups versus Cont group. $^{b}P < 0.05$, other groups versus CNI group. $^{c}P < 0.05$, other groups versus ADSC group. α-SMA: alpha-smooth muscle actin; β III tubulin: Tubb3 protein; CD31: platelet endothelial cell adhesion molecule-1; GAPDH: glyceraldehyde-3-phosphate dehydrogenase; MagADSC: magnetic field-assisted nanotechnology-treated ADSC; ADSC: adipose-derived stem cell; Cont: control; CNI: cavernous nerve injury.

The signal acquisition of the luciferin-luciferase reaction is influenced by the distance from the cell to the body surface, with deeper locations of cells showing a weaker signal. Thus, the different distributions of muscle, fat, and fur in the rat body may have affected signal collection and led to possible errors. Second, we observed a positive effect on erectile function after decreasing the ICI dosage from 1×10^6 to 2×10^5 cells, but did not determine whether these two injection dosages showed similar effects. The 12-week-old rats did not achieve full growth of the CC, and growth effects may have had synergistic effects on tissue regeneration; thus, whether these results apply in adult rats requires further analysis. At last, since CNI-related ED has been widely acknowledged and the skill of surgeons differs from each other, a CNI can be seen from mild to severe in the clinical setting; so far, there is no perfect animal model to reflect such condition. In the present study, we used the clamping model which has been proved to be effective in previous literature.[10] Further study will be needed to figure out a better model to simulate the real clinical scenario.

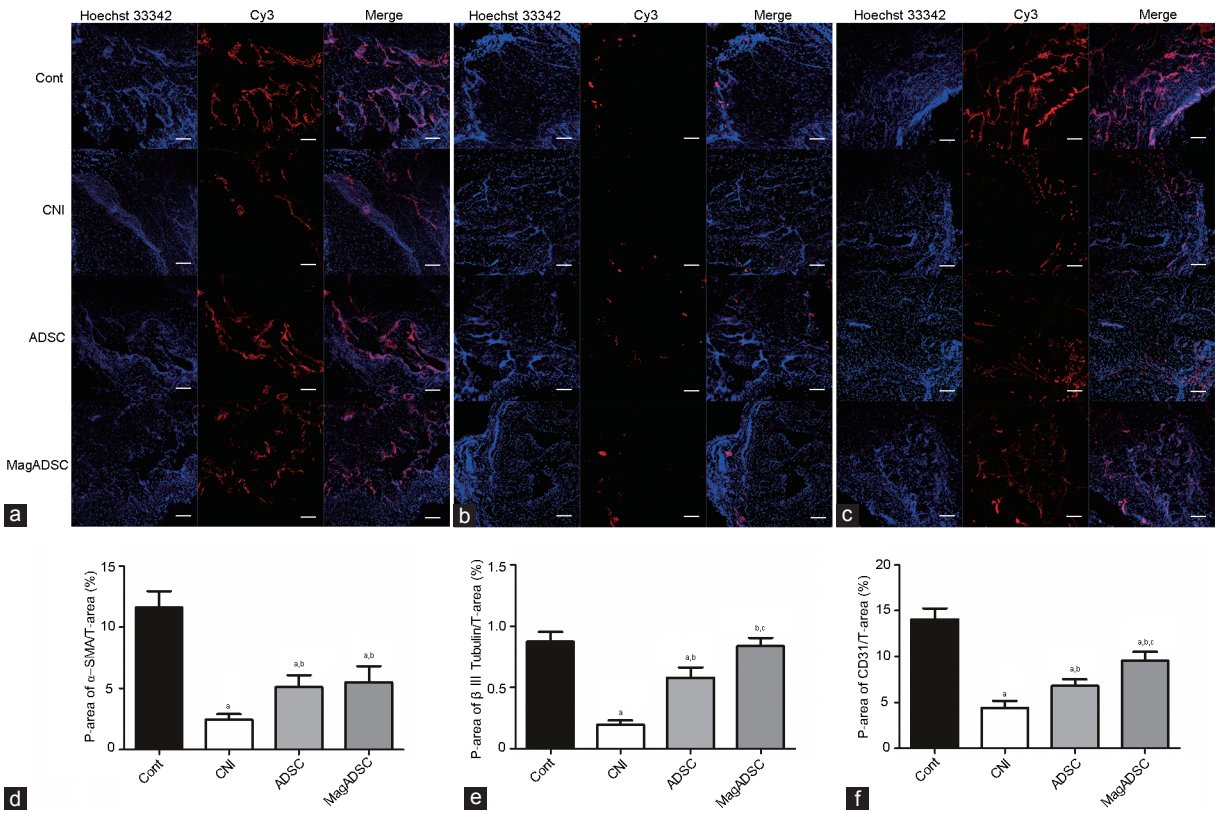

Figure 6: Smooth muscle, nerve, and endothelial contents in the CC. Immunohistochemical staining of (**a**) α-SMA in the smooth muscle, (**b**) β III tubulin in the nerve, and (**c**) CD31 in the endothelium. Statistical charts showing Cy3-positive areas of (**d**) α-SMA, (**e**) β III tubulin, and (**f**) CD31 in each group. Scale bars = 100 μm. $^{a}P < 0.05$, other groups versus Cont group. $^{b}P < 0.05$, other groups versus CNI group. $^{c}P < 0.05$, other groups versus ADSC group. Cont: control; CNI: cavernous nerve injury; ADSC: adipose-derived stem cell; MagADSC: magnetic field-assisted nanotechnology-treated ADSC; α-SMA: alpha-smooth muscle actin; β III tubulin: Tubb3 protein. P-area: positive area; T-area: total area.

CONCLUSION

Using an assisted magnetic field, a lower dosage ICI of NanoADSCs improved erectile function in BCNC rats and showed better effects than ICI of ADSCs. *In vivo* cell tracking revealed dynamic systemic diffusion of injected cells after ICI, and NanoADSCs had rather mild signal attenuation, suggesting that nanotechnology facilitated the colonization of ICI cells in CC and that a larger number of NanoADSCs survived in CC *in vivo* for at least 3 days after ICI.

AUTHOR CONTRIBUTIONS

HW, HTZ, and ZZ prepared the model animals. HW and HCL performed cell tracking experiments and wrote the manuscript; HJ, HCL, and KH worked on the design of the study. HJ, WHT, LMZ, DFL, and YZY contributed to drafting of the manuscript. All authors read and approved the final manuscript.

COMPETING INTERESTS

The authors declared no competing interests.

ACKNOWLEDGMENTS

This research was supported by the Beijing Natural Science Foundation (Grant No. 7174362) and the National Natural Science Foundation of China (Grant No. 81601272).

Supplementary information is linked to the online version of the paper on the *Asian Journal of Andrology* website.

REFERENCES

1 Siegel RL, Miller KD, Jemal A. Cancer statistics, 2016. *CA Cancer J Clin* 2016; 66: 7–30.
2 Bill-Axelson A, Holmberg L, Filen F, Ruutu M, Garmo H, *et al.* Radical prostatectomy versus watchful waiting in localized prostate cancer: the Scandinavian prostate cancer group-4 randomized trial. *J Natl Cancer Inst* 2008; 100: 1144–54.
3 Martinez-Salamanca JI, La Fuente JM, Fernandez A, Martinez-Salamanca E, Pepe-Cardoso AJ, *et al.* Nitrergic function is lost but endothelial function is preserved in the corpus cavernosum and penile resistance arteries of men after radical prostatectomy. *J Sex Med* 2015; 12: 590–9.
4 Resnick MJ, Koyama T, Fan KH, Albertsen PC, Goodman M, *et al.* Long-term functional outcomes after treatment for localized prostate cancer. *N Engl J Med* 2013; 368: 436–45.
5 Ficarra V, Novara G, Artibani W, Cestari A, Galfano A, *et al.* Retropubic, laparoscopic, and robot-assisted radical prostatectomy: a systematic review and cumulative analysis of comparative studies. *Eur Urol* 2009; 55: 1037–63.
6 Albersen M, Kendirci M, Van der Aa F, Hellstrom WJ, Lue TF, *et al.* Multipotent stromal cell therapy for cavernous nerve injury-induced erectile dysfunction. *J Sex Med* 2012; 9: 385–403.
7 Lin CS, Xin Z, Dai J, Huang YC, Lue TF. Stem-cell therapy for erectile dysfunction. *Expert Opin Biol Ther* 2013; 13: 1585–97.
8 Reed-Maldonado AB, Lue TF. The current status of stem-cell therapy in erectile dysfunction: a review. *World J Mens Health* 2016; 34: 155–64.
9 Lin CS, Xin ZC, Wang Z, Deng C, Huang YC, *et al.* Stem cell therapy for erectile dysfunction: a critical review. *Stem Cells Dev* 2012; 21: 343–51.
10 Lin H, Dhanani N, Tseng H, Souza GR, Wang G, *et al.* Nanoparticle improved stem cell therapy for erectile dysfunction in a rat model of cavernous nerve injury. *J Urol* 2016; 195: 788–95.
11 Bourin P, Bunnell BA, Casteilla L, Dominici M, Katz AJ, *et al.* Stromal cells from the adipose tissue-derived stromal vascular fraction and culture expanded adipose tissue-derived stromal/stem cells: a joint statement of the International Federation for Adipose Therapeutics and Science (IFATS) and the International Society for Cellular Therapy (ISCT). *Cytotherapy* 2013; 15: 641–8.
12 Mullerad M, Donohue JF, Li PS, Scardino PT, Mulhall JP. Functional sequelae of cavernous nerve injury in the rat: is there model dependency. *J Sex Med* 2006; 3: 77–83.
13 Ning H, Liu G, Lin G, Garcia M, Li LC, *et al.* Identification of an aberrant cell line among human adipose tissue-derived stem cell isolates. *Differentiation* 2009; 77: 172–80.
14 Desai VD, Hsia HC, Schwarzbauer JE. Reversible modulation of myofibroblast differentiation in adipose-derived mesenchymal stem cells. *PLoS One* 2014; 9: e86865.
15 Yiou R, Hamidou L, Birebent B, Bitari D, Le Corvoisier P, *et al.* Intracavernous injections of bone marrow mononucleated cells for postradical prostatectomy erectile dysfunction: final results of the INSTIN Clinical Trial. *Eur Urol Focus* 2017; 3: 643–5.
16 Xu Y, Guan R, Lei H, Li H, Wang L, *et al.* Therapeutic potential of adipose-derived stem cells-based micro-tissues in a rat model of postprostatectomy erectile dysfunction. *J Sex Med* 2014; 11: 2439–48.
17 Wankhade UD, Shen M, Kolhe R, Fulzele S. Advances in adipose-derived stem cells isolation, characterization, and application in regenerative tissue engineering. *Stem Cells Int* 2016; 2016: 3206807.
18 Albersen M, Fandel TM, Lin G, Wang G, Banie L, *et al.* Injections of adipose tissue-derived stem cells and stem cell lysate improve recovery of erectile function in a rat model of cavernous nerve injury. *J Sex Med* 2010; 7: 3331–40.
19 Zhu LL, Zhang Z, Jiang HS, Chen H, Chen Y, *et al.* Superparamagnetic iron oxide nanoparticle targeting of adipose tissue-derived stem cells in diabetes-associated erectile dysfunction. *Asian J Androl* 2017; 19: 425–32.
20 Chung CW, Marra KG, Li H, Leung AS, Ward DH, *et al.* VEGF microsphere technology to enhance vascularization in fat grafting. *Ann Plast Surg* 2012; 69: 213–9.
21 Kirkpatrick CJ, Unger RE, Krump-Konvalinkova V, Peters K, Schmidt H, *et al.* Experimental approaches to study vascularization in tissue engineering and biomaterial applications. *J Mater Sci Mater Med* 2003; 14: 677–81.
22 Xing Z, Xue Y, Finne-Wistrand A, Yang ZQ, Mustafa K. Copolymer cell/scaffold constructs for bone tissue engineering: co-culture of low ratios of human endothelial and osteoblast-like cells in a dynamic culture system. *J Biomed Mater Res A* 2013; 101: 1113–20.
23 Deng M, Gu Y, Liu Z, Qi Y, Ma GE, *et al.* Endothelial differentiation of human adipose-derived stem cells on polyglycolic acid/polylactic acid mesh. *Stem Cells Int* 2015; 2015: 350718.
24 Baglio SR, Rooijers K, Koppers-Lalic D, Verweij FJ, Perez Lanzon M, *et al.* Human bone marrow-and adipose-mesenchymal stem cells secrete exosomes enriched in distinctive miRNA and tRNA species. *Stem Cell Res Ther* 2015; 6: 127.
25 Lin G, Qiu X, Fandel T, Banie L, Wang G, *et al.* Tracking intracavernously injected adipose-derived stem cells to bone marrow. *Int J Impot Res* 2011; 23: 268–75.
26 Steffen F, Smolders LA, Roentgen AM, Bertolo A, Stoyanov J. Bone marrow-derived mesenchymal stem cells as autologous therapy in dogs with naturally occurring intervertebral disc disease: feasibility, safety, and preliminary results. *Tissue Eng Part C Methods* 2017; 23: 643–51.
27 Turco MP, de Souza AB, de Campos Sousa I, Fratini P, Veras MM, *et al.* Periurethral muscle-derived mononuclear cell injection improves urethral sphincter restoration in rats. *Neurourol Urodyn* 2017; 36: 2011–8.
28 Li H, Liu D, Li C, Zhou S, Tian D, *et al.* Exosomes secreted from mutant-HIF-1 alpha-modified bone-marrow-derived mesenchymal stem cells attenuate early steroid-induced avascular necrosis of femoral head in rabbit. *Cell Biol Int* 2017; 41: 1379–90.
29 Lee AS, Tang C, Rao MS, Weissman IL, Wu JC. Tumorigenicity as a clinical hurdle for pluripotent stem cell therapies. *Nat Med* 2013; 19: 998–1004.
30 Wang D, Wang S, Shi C. Update on cancer related issues of mesenchymal stem cell-based therapies. *Curr Stem Cell Res Ther* 2012; 7: 370–80.
31 Fandel TM, Albersen M, Lin G, Qiu X, Ning H, *et al.* Recruitment of intracavernously injected adipose-derived stem cells to the major pelvic ganglion improves erectile function in a rat model of cavernous nerve injury. *Eur Urol* 2012; 61: 201–10.

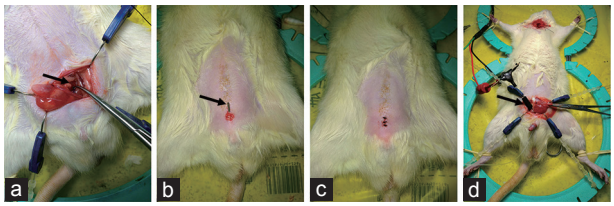

Supplementary Figure 1: CNI modeling, subcutaneous implantation of magnetic rod, and stimulation of erection. (**a**) A fine-tip hemostat clipping the left-sided CN; arrow indicates the nerve. (**b** and **c**) Magnetic rod subcutaneous implantation; arrow indicates the magnetic rod. (**d**) Erectile function assessment under electronic stimulation of CN; arrow indicates the stimulation hook. CN: cavernous nerve.

Supplementary Table 1: Intracavernous pressure and mean arterial pressure values of each group (mean±standard error of the mean)

Group	*Mean peak ICP (mmHg)*	*ICP/MAP (%)*	*Total ICP (mmHg)*
Cont	95.41±3.3	55.79±3.0	3433.26±101.3
CNI	36.00±0.8*	24.58±2.9*	621.80±19.4*
ADSC	60.81±4.4$^{*,\#}$	37.29±3.9$^{*,\#}$	1635.17±119.7$^{*,\#}$
MagADSC	85.69±4.3$^{\#,\S}$	49.34±4.1$^{\#,\S}$	3172.97±76.0$^{\#,\S}$

$^{*}P<0.05$ compared to Cont; $^{\#}P<0.05$ compared to CNI; $^{\S}P<0.05$ compared to ADSC. Cont: normal control group; CNI: cavernous nerve injury group; ADSC: adipose-derived stem cell-treated group; MagADSC: magnetic field-assisted group; ICP: intracavernous pressure; MAP: mean arterial pressure